DOI: 10.20858/tp.2025.20.3.14

**Keywords:** imbalance; turbocharger; marine propulsion units; bearings; dynamic stability; numerical methods

Aleksander MAZURKOW<sup>1</sup>, Wojciech HOMIK<sup>2</sup>, Marcin MATUSZAK<sup>3</sup>\*

# ANALYSIS OF SELECTED CASES OF IMBALANCE AND DYNAMIC PROPERTIES OF TURBOCHARGER ROTATING ASSEMBLIES

**Summary.** The efficiency and reliability of the propulsion system of, for example, a vessel equipped with a supercharged combustion engine, largely depend on a properly working turbocharger. Despite the use of a sophisticated bearing system and a turbocharger rotating assembly, its constructors struggle with ensuring its dynamic stability. This study presents a dynamic model of a turbocharger rotating system, along with the corresponding numerical calculations. The model addresses the issue of vibration damping in non-locating plain bearings and its impact on the rotating unit of the turbocharger. As a result of numerical calculations, the areas of stable operation of the rotating unit were obtained. It can be concluded that the floating ring bearings used in the turbocharger effectively suppress the vibroacoustic effects accompanying the operating rotating assembly. Furthermore, the analyses indicate that the causes of turbocharger malfunction can be attributed to excessive imbalance in the rotating assembly and the improper stiffness of the rotating unit. The presented research may be beneficial in practice, providing insight into how to extend the service life of not only the power unit itself, but also the turbocharger.

## 1. INTRODUCTION

Turbochargers provide greater power and efficiency to multi-cylinder internal combustion engines, which serve as the main and auxiliary propulsion systems of marine vessels [1-3] (Fig. 1). The basic assembly that determines the proper operation of turbochargers is the rotating assembly, which consists of a shaft, turbine, and compressor rotors. This assembly is supported by slide bearings, which, in addition to their primary function, dampen vibrations. C0-45 turbochargers use slide bearings with a floating ring operating under hydrodynamic lubrication conditions. These bearings differ from their conventional counterparts in that they have an additional ring called a floating ring, which is loosely fitted between the shaft journal and the fixed bearing ring (outer ring).

A number of studies have been conducted to ensure the optimal design of turbochargers, particularly in terms of their reliability, and their results are used by designers. An analysis of the available literature shows that turbocharger tests are carried out on complete turbochargers, rotating assemblies, and individual parts, such as bearings. It is worth noting that the authors of these studies provided only a limited discussion of their results.

Two main directions can be distinguished in bearing research. The first is research conducted in the area of static balance [4-8], and the second is research conducted in the area of dynamic balance. The research models of bearings with floating rings, both in static and dynamic equilibrium, take into account the fact that the external load is transferred by hydrodynamic forces generated in external and internal

<sup>&</sup>lt;sup>1</sup> Rzeszów University of Technology, al. Powstańców Warszawy 12, 35-959 Rzeszów, Poland; e-mail: almaz@prz.edu.pl; orcid.org/0000-0003-1719-991

<sup>&</sup>lt;sup>2</sup> Rzeszów University of Technology, al. Powstańców Warszawy 12, 35-959 Rzeszów, Poland; e-mail: whomik@prz.edu.pl; orcid.org/0000-0001-7843-7761

<sup>&</sup>lt;sup>3</sup> Maritime University of Szczecin; Wały Chrobrego 1-2, 70-500 Szczecin, Poland; e-mail: m.matuszak@pm.szczecin.pl; orcid.org/ 0000-0002-1746-6814

<sup>\*</sup> Corresponding author. E-mail: <u>m.matuszak@pm.szczecin.pl</u>

oil films. For the purpose of analysing heat transfer in bearings with floating rings, isothermal, adiabatic, and diathermic models are used. A previous paper [8] presents the results of research on the adiabatic heat transfer model in bearings. In this model, the temperature of the external and internal oil films was determined based on heat balances, taking into account the circumferential and axial oil flow. Moreover, the paper presents selected results of turbocharger tests carried out on a test bench. The results of the tests show that the floating ring of the bearing operates unsteadily and the rotating system generates vibrations [11-14], which directly affect the durability and reliability of the turbocharger. Additionally, bench tests have demonstrated that the durability and reliability of the turbocharger also depend on the geometric parameters of the bearings. However, labor-intensive and costly research efforts have not provided answers to many questions troubling researchers, especially those concerning bearings with floating rings.

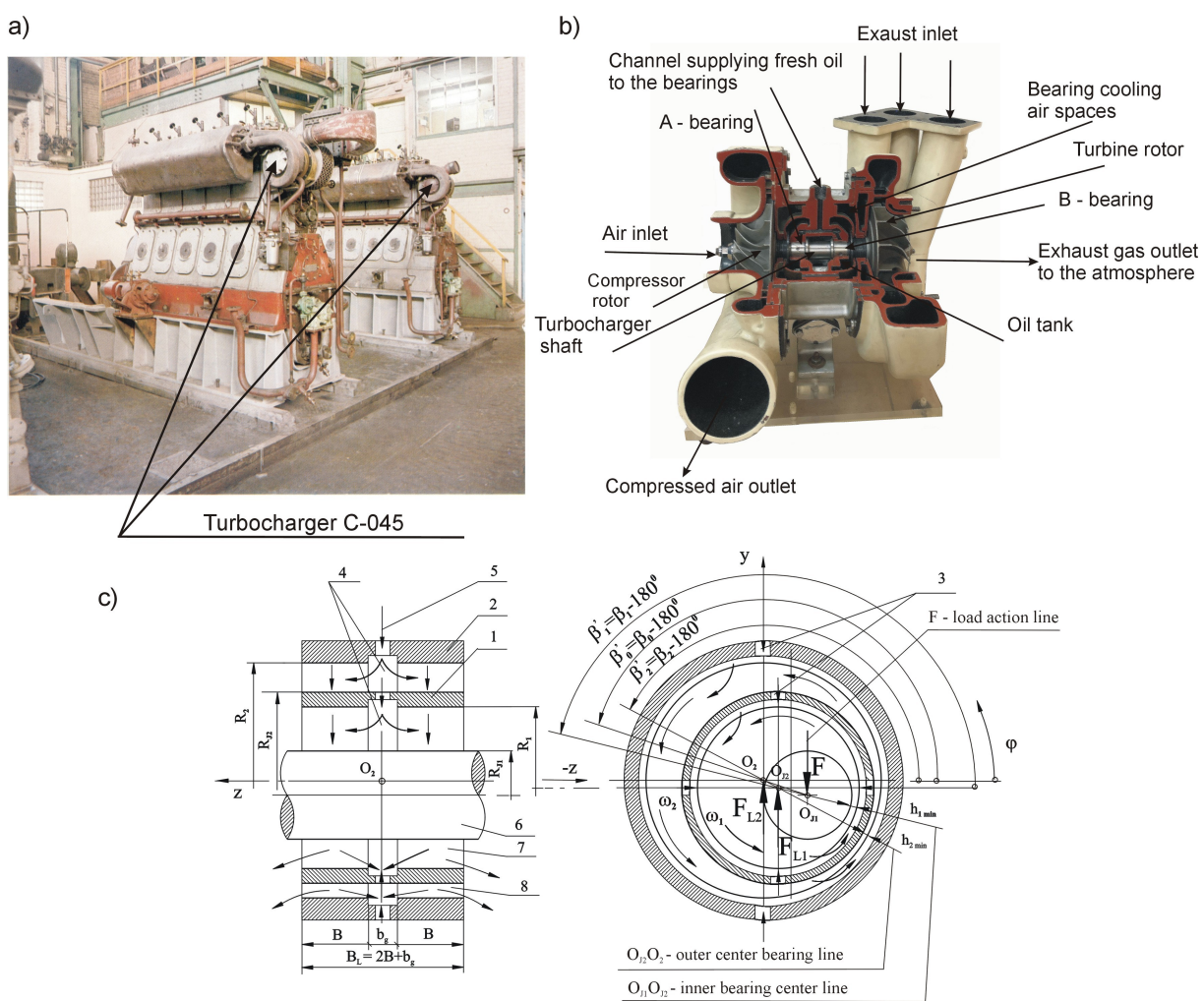


Fig. 1. a) Sulzer 5BAH22 engine, b) Turbocharger CO-45, c) Slide bearing with a floating ring: 1 – floating ring, 2 – fixed bearing bush, 3 – holes, 4 – circumferential groove, 5 – direction of oil flow, 6 – journal, 7 – internal oil film (i=1), 8 – external oil film (i=2)

Bearing this in mind, the authors of this paper developed a dynamic model of a floating ring bearing. In this model, they assumed the actual mass and geometric dimensions of the C0-45 turbocharger, as well as that the fluid is a viscoelastic fluid whose viscosity changes with temperature. The model was described by an appropriate set of differential equations, enabling a series of tests on the dynamics of the turbocharger rotating system and the influence of the operating turbocharger on the power of the drive unit. It is worth noting that the theoretical results of the tests were verified on a test bench.

Based on the analysis of the test results, the authors concluded that the vibrations of the turbocharger rotating assembly at sub-synchronous frequencies result from the instability of oil flow in the bearings, the difference in the operating parameters of the external and internal oil films, and the geometric characteristics of the floating bearing ring. The detailed test results are discussed in papers [15-17]. As mentioned above, research on turbochargers covers many issues, but to the authors' knowledge, it rarely addresses the phenomena related to vibration damping in sliding bearings with floating rings. Thus, the authors conducted relevant tests on the C0-45 turbocharger used in marine propulsion systems. The results presented in this paper have many important theoretical and practical implications, which the authors believe will fill a gap in the literature on research into phenomena related to ensuring the dynamic stability of turbochargers.

### 2. DETERMINATION OF STIFFNESS AND DAMPING COEFFICIENTS

As indicated by the available literature, to study the dynamic properties of an oil film, it is necessary to know the stiffness and damping coefficients [10]. For a reference system described by the XYZ coordinates (Figure 2), the coefficients  $c_{xy}$  and  $d_{xy}$  describe the stiffness and vibration damping capacity for displacements on the OXZ plane and the OYZ plane, while  $c_{xx}$ ,  $d_{xx}$  describe stiffness and vibration damping capacity for displacements on the OXZ plane, taking into account the influence forces on the OXZ plane. Meanwhile,  $c_{yx}$ ,  $d_{yx}$  represent stiffness and vibration damping capacity for displacements on the OYZ plane, taking into account the influence of forces on the OXZ plane. Finally,  $c_{yy}$ ,  $d_{yy}$  indicate stiffness and vibration damping for displacements on the OYZ plane, taking into account the influence of forces on the OYZ plane.

These coefficients can be presented in dimensionless form as follows:

$$c_{xx}^{*} = \frac{c_{xx}}{\alpha_{ki}}, c_{xy}^{*} = \frac{c_{xy}}{\alpha_{ki}}, c_{yx}^{*} = \frac{c_{yx}}{\alpha_{ki}}, c_{yy}^{*} = \frac{c_{yy}}{\alpha_{ki}},$$

$$d_{xx}^{*} = \frac{d_{xx}}{\alpha_{bi}}, d_{xy}^{*} = \frac{d_{xy}}{\alpha_{bi}}, d_{yx}^{*} = \frac{d_{yx}}{\alpha_{bi}}, d_{yy}^{*} = \frac{d_{yy}}{\alpha_{bi}},$$

$$\eta_{0} \cdot \omega_{i} \cdot B \qquad \eta_{0} \cdot \omega_{i}^{2} \cdot B$$
(1)

where:  $\alpha_{ki} = \frac{\eta_0 \cdot \omega_i \cdot B}{2 \cdot \psi_i^2}$ ,  $\alpha_{bi} = \frac{\eta_0 \cdot \omega_i^2 \cdot B}{2 \cdot \psi_i^2}$ 

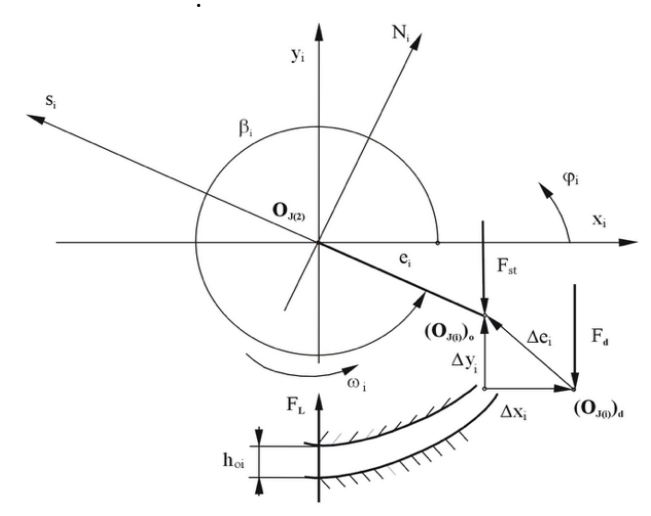


Fig. 2. The system of forces in the bearing in the dynamic equilibrium position, where i = 1 – inner oil film, i = 2 – outer oil film,  $(O_{J(i)})_o$  – static equilibrium position,  $(O_{J(i)})_d$  – dynamic equilibrium position,  $O_{J1}$  – center of the shaft journal of the rotating assembly,  $O_{J2}$  – center of the floating ring,  $O_2$  – center of the fixed ring, for i = 1  $O_{J(i)} = O_{J1}$  and  $O_{J(2)} = O_{J2}$ , for i = 2  $O_{J(i)} = O_{J2}$  and  $O_{J(2)} = O_2$ , SON – reference system related to the center of the journal, floating ring and fixed ring, XOY – basic reference system

The coefficients above can be determined based on the linearization of lift in the dynamic equilibrium position or the linearization of pressure near the dynamic equilibrium.

To determine the stiffness and damping coefficients, the authors used the method of pressure linearization in the position of dynamic balance. Linearization of the pressure function can be carried out by expanding the pressure function in the Taylor series at the position of dynamic balance  $p_d = p_d(x,z)$ , while maintaining the terms containing the first derivatives:

$$p_{di} = p_{oi} + \left(\frac{\partial p}{\partial x_{oi}}\right)_{d} \Delta x_{i} + \left(\frac{\partial p}{\partial y_{oi}}\right)_{d} \Delta y_{i} + \left(\frac{\partial p}{\partial \dot{x}_{oi}}\right)_{d} \Delta \dot{x}_{i} + \left(\frac{\partial p}{\partial \dot{y}_{oi}}\right)_{d} \Delta \dot{y}_{i}$$
(2)

where: o – a static reference system related to a journal or a floating ring, i=1 – internal oil film, i=2 – external oil film, d – reference system related to static/dynamic balance.

The development described by Equation (2) is correct for small vibrations of the journal and the floating ring around the balance position, in which the local change in the viscosity value caused by the change in the height of the lubrication gaps is negligibly small.

The equations of excess hydrodynamic force take the form described by Equation (3).

$$\Delta F_{Li} = \begin{bmatrix} \Delta F_{Lxi} \\ \Delta F_{Lyi} \end{bmatrix} = \begin{bmatrix} F_{cxi} + F_{dxi} \\ F_{cyi} + F_{dyi} \end{bmatrix} = \begin{bmatrix} c_{xxi} & c_{xyi} \\ c_{yxi} & c_{yyi} \end{bmatrix} \begin{bmatrix} \Delta x_i \\ \Delta y_i \end{bmatrix} + \begin{bmatrix} d_{xxi} & d_{xyi} \\ d_{yxi} & d_{yyi} \end{bmatrix} \begin{bmatrix} \Delta \dot{x}_i \\ \Delta \dot{y}_i \end{bmatrix}$$
(3)

The stiffness and damping coefficients presented in dimensional form are

$$c_{xxi} = \sin \beta_{i} \int_{-B/2}^{B/2} \int_{0}^{2\pi} \left( \frac{\partial p_{i}}{\partial x_{si}} \right)_{o} (\cos \varphi_{i} + \sin \varphi_{i}) R_{i} d\varphi_{i} dz,$$

$$c_{xyi} = \sin \beta_{i} \int_{-B/2}^{B/2} \int_{0}^{2\pi} \left( \frac{\partial p_{i}}{\partial y_{si}} \right)_{o} (\cos \varphi_{i} + \sin \varphi_{i}) R_{i} d\varphi_{i} dz,$$

$$c_{yxi} = \cos \beta_{i} \int_{-B/2}^{B/2} \int_{0}^{2\pi} \left( \frac{\partial p_{i}}{\partial x_{si}} \right)_{o} (\cos \varphi_{i} + \sin \varphi_{i}) R_{i} d\varphi_{i} dz,$$

$$c_{yyi} = \cos \beta_{i} \int_{-B/2}^{B/2} \int_{0}^{2\pi} \left( \frac{\partial p_{i}}{\partial y_{si}} \right)_{o} (\cos \varphi_{i} + \sin \varphi_{i}) R_{i} d\varphi_{i} dz,$$

$$d_{xxi} = \sin \beta_{i} \int_{-B/2}^{B/2} \int_{0}^{2\pi} \left( \frac{\partial p_{i}}{\partial \dot{x}_{si}} \right)_{o} (\cos \varphi_{i} + \sin \varphi_{i}) R_{i} d\varphi_{i} dz,$$

$$d_{xyi} = \sin \beta_{i} \int_{-B/2}^{B/2} \int_{0}^{2\pi} \left( \frac{\partial p_{i}}{\partial \dot{y}_{si}} \right)_{o} (\cos \varphi_{i} + \sin \varphi_{i}) R_{i} d\varphi_{i} dz,$$

$$d_{yxi} = \cos \beta_{i} \int_{-B/2}^{B/2} \int_{0}^{2\pi} \left( \frac{\partial p_{i}}{\partial \dot{x}_{si}} \right)_{o} (\cos \varphi_{i} + \sin \varphi_{i}) R_{i} d\varphi_{i} dz,$$

$$d_{yyi} = \cos \beta_{i} \int_{-B/2}^{B/2} \int_{0}^{2\pi} \left( \frac{\partial p_{i}}{\partial \dot{x}_{si}} \right)_{o} (\cos \varphi_{i} + \sin \varphi_{i}) R_{i} d\varphi_{i} dz,$$

$$d_{yyi} = \cos \beta_{i} \int_{-B/2}^{B/2} \int_{0}^{2\pi} \left( \frac{\partial p_{i}}{\partial \dot{x}_{si}} \right)_{o} (\cos \varphi_{i} + \sin \varphi_{i}) R_{i} d\varphi_{i} dz,$$

The bearing model in the static balance position is described by the following quantities:

relative eccentricity, determined by the relationship:

$$\varepsilon_i = \frac{e_i}{C_{R_i}} \tag{5}$$

The Sommerfeld number, which is:

for the internal oil film 
$$S_{o1} = \frac{\eta_{eff} \cdot (\omega_1 + \omega_2) \cdot D_1 \cdot B}{F_L} \left(\frac{R_1}{C_{R1}}\right)^2$$
 (6)

for the external oil film 
$$S_{o2} = \frac{\eta_{eff} \cdot \omega_2 \cdot D_2 \cdot B}{F_L} \left(\frac{R_3}{C_{R2}}\right)^2$$

In the dynamic model, the relationship between the Sommerfeld number  $S_{oi}$ , and the relative eccentricity  $\varepsilon_i$  was determined from the balance condition between the components coming from the static bearing load F and the load capacity of the oil film  $F_L$ . This relationship can be presented in a dimensionless form:

$$\begin{aligned}
f_{si} &= \frac{F_{si}}{F} \\
f_{\varphi i} &= \frac{F_{\varphi i}}{F}
\end{aligned} = \left(\frac{B_{i}}{D_{i}}\right)^{2} S_{oi} \int_{\varphi_{A}}^{\varphi_{B}} \frac{1}{h_{i}^{*3}} \left(\varepsilon_{i} (1 - 2\dot{\varphi}_{i}) \sin \varphi_{i} - 1\dot{\varepsilon}_{i} \cos \varphi_{i}\right) \left\{-\cos \varphi_{i} \atop \sin \varphi_{i}\right\} d\varphi_{i} \tag{7}$$

where:  $\dot{\varepsilon}_i = \frac{1}{\omega_i} \frac{d\varepsilon_i}{dt}$ ,  $\dot{\varphi}_i = \frac{1}{\omega_i} \frac{d\varphi_i}{dt}$ 

For static balance conditions when  $\varepsilon_t = (\varepsilon)_0$ ,  $(\varphi_i) = (\varphi)_0$ , and  $\dot{\varepsilon}_i = \dot{\varphi}_i = 0$  between the forces of the oil film expressed in a dimensionless form, there is a relation:

$$(f_{si})_0^2 + (f_{vi})_0^2 = 1$$
 (8)

### 3. DISCRETE MODEL OF A TURBOCHARGER ROTATING SYSTEM

A discrete model of the rotating assembly (shown in Fig. 3) was developed to study the impact of the above-mentioned factors on the operation of the turbocharger.

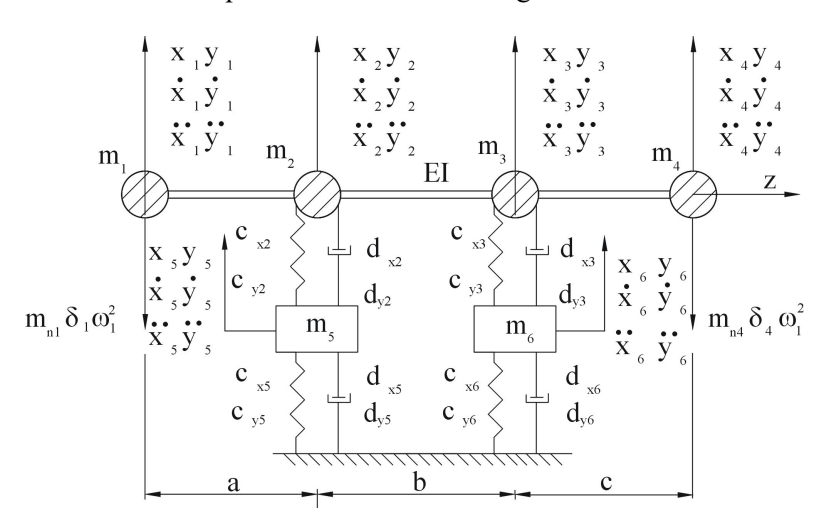


Fig. 3. Discrete Dynamic model of the turbocharger rotating assembly with bearings [10] where:  $m_1 
dots m_6 - 1$  concentrated masses,  $c_x$ ,  $c_y$  – stiffness coefficients,  $d_x$ ,  $d_y$  - damping coefficients, E – Young's modulus, I – moment of inertia,  $m_{n1}$ ,  $m_{n4}$  – imbalance of the rotating masses,  $m_{n1} \cdot \delta_1 \cdot \omega_1^2$ ,  $m_{n4} \cdot \delta_4 \cdot \omega_1^2$  – forces resulting from mass imbalance, a, b, c – distance between concentrated masses

The equations of motion written in matrix form on the OXZ and OYZ planes are as follows:

$$[M_{x}] \cdot [\ddot{x}] + [D_{xx}] \cdot [\dot{x}] + [D_{xy}] \cdot [\dot{x}] + [C_{xx}] \cdot [x] + [C_{xy}] \cdot [x] = [F_{x}(t)],$$

$$[M_{y}] \cdot [\ddot{y}] + [D_{yy}] \cdot [\dot{y}] + [D_{yx}] \cdot [\dot{y}] + [C_{yy}] \cdot [y] + [C_{yx}] \cdot [y] = [F_{y}(t)]$$
(9)

The stability of the rotary unit was assessed based on the Hurwitz criterion. According to this criterion, the necessary and sufficient conditions for the stability of the assembly are that all the real parts of the roots of the characteristic equation are negative.

# 4. NUMERICAL CALCULATIONS

10. Bearing oil pressure:  $p_z = 0.1$  MPa

The areas of stable operation of the rotating unit were determined in three stages. In the first stage, in the balancing position, the following were determined: the load capacity of the oil film  $F_L$ , the relative bearing eccentricity  $\varepsilon_1$ , height of the oil film  $h_i(x)$ , pressure  $p_i(x,z)$ , and temperature distributions  $T_i(x,z)$  in the oil films. In the second stage, for the dynamic equilibrium position determined by the eccentricities  $\varepsilon_l$  and  $\varepsilon_2$ , the values of the bearing stiffness coefficients  $c_{ix,y}$  and damping coefficients  $d_{ix,y}$  were determined. In the third stage, the area of stable operation of the rotating unit, including bearing supports, was determined.

The values used for the numerical calculation of the rotating turbocharger unit are shown in Table 1.

Table 1

# Set parameters

1. Inner diameter of the inner and outer bearing rings:  $D_1 = 31.752, D_2 = 37.986 \text{ mm},$ radial clearance quotient:  $C_R^*=C_{R2}/C_{RI}=0.5$ , 1.12, 2.0, bearing width: *B*=8.71 mm 2. Geometric parameters of the rotating assembly: <u>a=0.055 [m], b=0.075 [m], c=0.045 [m],  $I_x$ =0.15·10<sup>-6</sup> [m<sup>4</sup>]</u> 3. Relative eccentricity:  $\varepsilon_2 = <0.3-0.8>$ 4. Bearing ring rotational speed  $N_{J1}$ =<26,000–42,000>RPM 5. Oil viscosity:  $\eta(T) = 0.184 \cdot e^{-55291\cdot10^{-6}(T-20)+239\cdot10^{-6}(T-20)^2}$  Pa·s Oil density:  $\rho(T) = 896.25 - 1.4375 \cdot T + 6.25 \cdot 10^{-3} \cdot T^2 \text{ kg/m}^3$ Specific heat:  $c_p(T) = 1802.07 - 2.878 \cdot T + 0.0087 \cdot T^2 \text{ J/kg} \cdot ^{\circ}\text{C}$ Thermal conductivity of the oil:  $\lambda$ =0.145 J/kg·°C 6. Young's modulus of elasticity: E=1.915·10<sup>11</sup> N/m<sup>2</sup> 7. Concentrated masses:  $m_1=5.0$ ,  $m_2=0.3$ ,  $m_3=0.25$ ,  $m_4=2.0$ ,  $m_5=m_6=0.055$  N·s<sup>2</sup>/m 8. Imbalances of rotating masses:  $N_{w1} = <0 - 3.8 \cdot 10^{-5} >, N_{w4} = <0 - 2.5 \cdot 10^{-5} > \text{kg} \cdot \text{m}$ 9. Ambient and bearing oil temperature:  $T_0 = 20$ ,  $T_z = 60$ °C

Tests were performed for both static and dynamic equilibrium positions. The position of the floating ring relative to the fixed ring, which was determined by the relative eccentricity  $\varepsilon_2$ , was taken as the setpoint. The scheme for solving the equations of the mathematical model is shown in Fig. 4.

For the static equilibrium position, m, in the following were calculated: hydrodynamic buoyancy force  $F_L$ , maximum temperature  $T_{1,2 max}$ , and oil film pressure  $p_{1,2 max}$ , as well as minimum oil film height  $h_{1,2 min}$ . Fig. 5 shows the effect of bearing journal speed  $N_{JI}$  and eccentricity  $\varepsilon_2$  on the hydrodynamic

buoyancy force, which was presented in the dimensionless form,  $F^*_{L1} = \frac{F_L \cdot \psi_1^2}{4 \cdot B \cdot R_1 \cdot (\omega_1 + \omega_2) \cdot \eta_0}$ , and

$$F^*_{L2} = \frac{F_L \cdot \psi_2^2}{4 \cdot B \cdot R_1 \cdot \omega_2 \cdot \eta_0}$$
, where  $\psi_{1,2} = \frac{C_{R1,2}}{R_{1,2}}$ . On the other hand, for the position of dynamic

equilibrium in the nodes of the rotating unit, the amplitudes of displacements and accelerations of vibrations  $x_{1,2,3,...6}, y_{1,2,3,...6}, a_{y_1,2,3,...,6}$ , were determined.

Calculations of the influence of the asymmetry of the turbine and compressor rotors and the rotational speed of the rotating unit on the vibration level were carried out for two selected sets of values:

I set:  $N_{w1}$ =3.8,  $N_{w4}$ =2.5 [kg·m],  $N_{J1}$ =26,000–42,000 RPM II set:  $N_{w1}$ =1.9,  $N_{w4}$ =1.25 [kg·m],  $N_{J1}$ =26,000–42,000 RPM

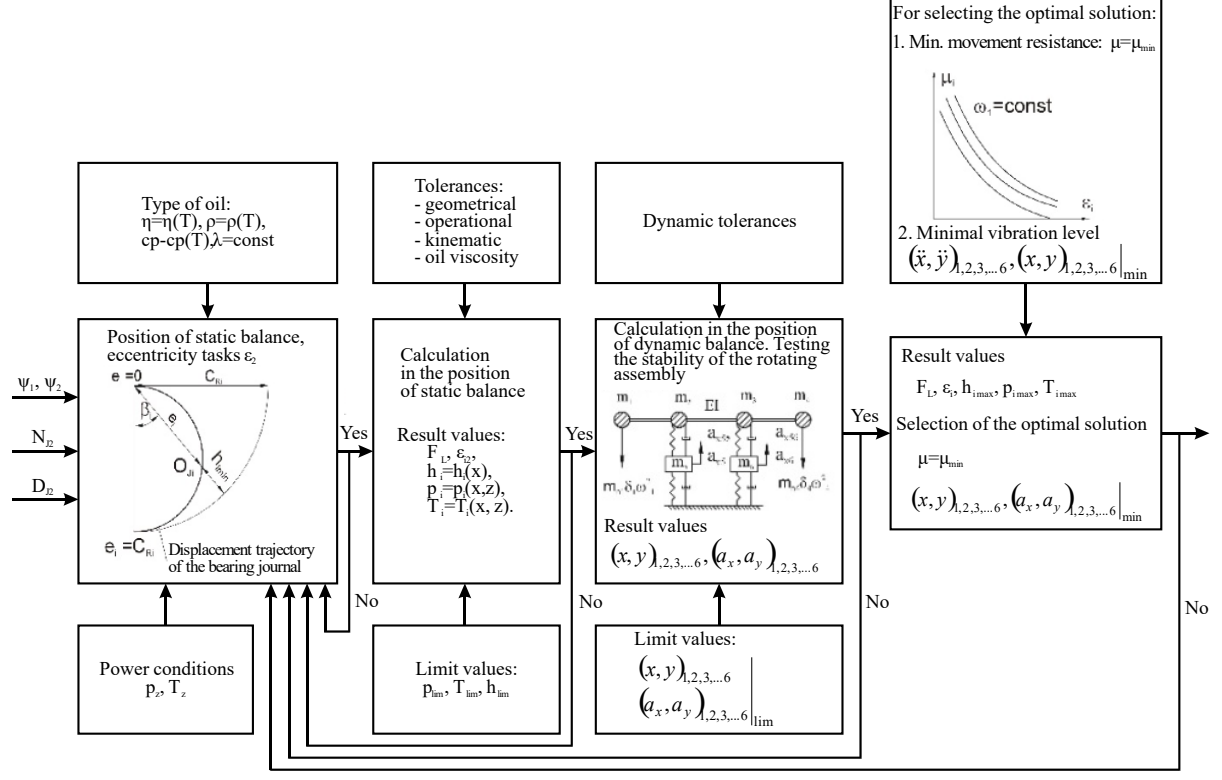


Fig. 4. Controlling the process of calculating the static and dynamic properties of turbocharger rotating assemblies

The displacement amplitudes are shown in Figs. 6 and 7, and the acceleration values that are related to the gravitational acceleration  $a_{x,y,1,2,3,...6}^* = \frac{a_{x,y,1,2,3,...6}}{g = 9.81 \text{ m/s}^2}$  are presented in (Fig. 8, 9).

From the results of the tests (Fig. 5) of dimensionless loads 
$$F^*_{L1} = \frac{F_L \cdot \psi_1^2}{4 \cdot B \cdot R_1 \cdot (\omega_1 + \omega_2) \cdot \eta_0} = F^*_{L1} (N_{J1}, \varepsilon_2), \quad F^*_{L2} = \frac{F_L \cdot \psi_2^2}{4 \cdot B \cdot R_1 \cdot \omega_2 \cdot \eta_0} = F^*_{L2} (N_{J1}, \varepsilon_2), \quad \text{if } F^*_{L2} = \frac{F_L \cdot \psi_2^2}{4 \cdot B \cdot R_1 \cdot \omega_2 \cdot \eta_0} = F^*_{L2} (N_{J1}, \varepsilon_2), \quad \text{if } F^*_{L3} = \frac{F_L \cdot \psi_2^2}{4 \cdot B \cdot R_1 \cdot \omega_2 \cdot \eta_0} = F^*_{L3} (N_{J1}, \varepsilon_2), \quad \text{if } F^*_{L3} = \frac{F_L \cdot \psi_2^2}{4 \cdot B \cdot R_1 \cdot \omega_2 \cdot \eta_0} = F^*_{L3} (N_{J1}, \varepsilon_2), \quad \text{if } F^*_{L3} = \frac{F_L \cdot \psi_2^2}{4 \cdot B \cdot R_1 \cdot \omega_2 \cdot \eta_0} = F^*_{L3} (N_{J1}, \varepsilon_2), \quad \text{if } F^*_{L3} = \frac{F_L \cdot \psi_2^2}{4 \cdot B \cdot R_1 \cdot \omega_2 \cdot \eta_0} = F^*_{L3} (N_{J1}, \varepsilon_2), \quad \text{if } F^*_{L3} = \frac{F_L \cdot \psi_2^2}{4 \cdot B \cdot R_1 \cdot \omega_2 \cdot \eta_0} = F^*_{L3} (N_{J1}, \varepsilon_2), \quad \text{if } F^*_{L3} = \frac{F_L \cdot \psi_2^2}{4 \cdot B \cdot R_1 \cdot \omega_2 \cdot \eta_0} = F^*_{L3} (N_{J1}, \varepsilon_2), \quad \text{if } F^*_{L3} = \frac{F_L \cdot \psi_2^2}{4 \cdot B \cdot R_1 \cdot \omega_2 \cdot \eta_0} = F^*_{L3} (N_{J1}, \varepsilon_2), \quad \text{if } F^*_{L3} = \frac{F_L \cdot \psi_2^2}{4 \cdot B \cdot R_1 \cdot \omega_2 \cdot \eta_0} = F^*_{L3} (N_{J1}, \varepsilon_2), \quad \text{if } F^*_{L3} = \frac{F_L \cdot \psi_2^2}{4 \cdot B \cdot R_1 \cdot \omega_2 \cdot \eta_0} = F^*_{L3} (N_{J1}, \varepsilon_2), \quad \text{if } F^*_{L3} = \frac{F_L \cdot \psi_2^2}{4 \cdot B \cdot R_1 \cdot \omega_2 \cdot \eta_0} = F^*_{L3} (N_{J1}, \varepsilon_2), \quad \text{if } F^*_{L3} = \frac{F_L \cdot \psi_2^2}{4 \cdot B \cdot R_1 \cdot \omega_2 \cdot \eta_0} = F^*_{L3} (N_{L3}, \varepsilon_2), \quad \text{if } F^*_{L3} = \frac{F_L \cdot \psi_2^2}{4 \cdot B \cdot R_1 \cdot \omega_2 \cdot \eta_0} = F^*_{L3} (N_{L3}, \varepsilon_2), \quad \text{if } F^*_{L3} = \frac{F_L \cdot \psi_2^2}{4 \cdot B \cdot R_1 \cdot \omega_2 \cdot \eta_0} = F^*_{L3} (N_{L3}, \varepsilon_2), \quad \text{if } F^*_{L3} = \frac{F_L \cdot \psi_2^2}{4 \cdot B \cdot R_1 \cdot \omega_2 \cdot \eta_0} = F^*_{L3} (N_{L3}, \varepsilon_2), \quad \text{if } F^*_{L3} = \frac{F_L \cdot \psi_2^2}{4 \cdot B \cdot R_1 \cdot \omega_2 \cdot \eta_0} = F^*_{L3} (N_{L3}, \varepsilon_2), \quad \text{if } F^*_{L3} = \frac{F_L \cdot \psi_2^2}{4 \cdot B \cdot R_1 \cdot \omega_2 \cdot \eta_0} = F^*_{L3} (N_{L3}, \varepsilon_2), \quad \text{if } F^*_{L3} = \frac{F_L \cdot \psi_2^2}{4 \cdot B \cdot R_1 \cdot \omega_2 \cdot \eta_0} = F^*_{L3} (N_{L3}, \varepsilon_2), \quad \text{if } F^*_{L3} = \frac{F_L \cdot \psi_2^2}{4 \cdot B \cdot R_1 \cdot \omega_2 \cdot \eta_0} = F^*_{L3} (N_{L3}, \varepsilon_2), \quad \text{if } F^*_{L3} = \frac{F_L \cdot \psi_2^2}{4 \cdot B \cdot R_1 \cdot \omega_2 \cdot \eta_0} = F^*_{L3} (N_{L3}, \varepsilon_2), \quad \text{if } F^*_{L3} = \frac{F_L \cdot \psi_2^2}{4 \cdot B \cdot R_1 \cdot \omega_2 \cdot \eta_0} = F^*_{L3} (N_{L3}, \varepsilon_2), \quad \text{if } F^*$$

can be observed that the position of the bearing journals and the inner and outer oil film has a significant effect on the amplitudes of vibration displacements in the direction of the x and y coordinates. The calculations show that for  $\varepsilon_2$ =0.85, the rotating assembly is stable in the whole tested speed range  $N_{J1} = \langle 26000 - 42000 \rangle$ RPM. On the other hand, for eccentricity  $\varepsilon_2$ =0.7 and 0.6, it is unstable over the entire tested velocity range.

The results of numerical studies shown in Figs. 6 and  $7x_{1,2,...6}(N_{J1}, \varepsilon_2 = 0.85)$  and  $y_{1,2,...6}(N_{J1}, \varepsilon_2 = 0.85)$  are increasing functions. Bearing nodes  $x_{5,6}$  and  $y_{5,6}$  have much lower acceleration amplitudes than turbine rotor and compressor nodes  $x_{1,4}$  and  $y_{1,4}$ . Reducing the asymmetry of the turbine and compressor rotors significantly reduces amplitudes  $x_{1,4}$  and displacements  $y_{1,4}$  in these nodes.

The mass of the turbine rotor is much greater than the mass of the compressor rotor. This increases vibration displacements on the compressor side, where  $x_4 > x_1$  and  $y_4 > y_1$ .

Similarly, for the research results described above, the courses (Figs. 8 and 9) of accelerations  $a_{x_1,2,...6}^*(N_{J1})$  and displacements  $y_{1,2,...6} = y_{1,2,...6}(N_{J1})$ , which are increasing functions, are presented.

The bearing nodes (5, 6) have much lower acceleration amplitudes than the rotor nodes—turbines and compressors (1, 4):  $a_{x5,6}^* < a_{x1,4}^*$  and  $a_{y5,6}^* < a_{y1,4}^*$   $y_{1,4}$ . As the calculations carried out for two sets of data show, the reduction of the imbalance of the rotors of the turbine and compressor reduces the acceleration amplitudes  $a_{x5,6}^*$ ,  $a_{y1,4}^*$ . The case under study involves a double reduction.

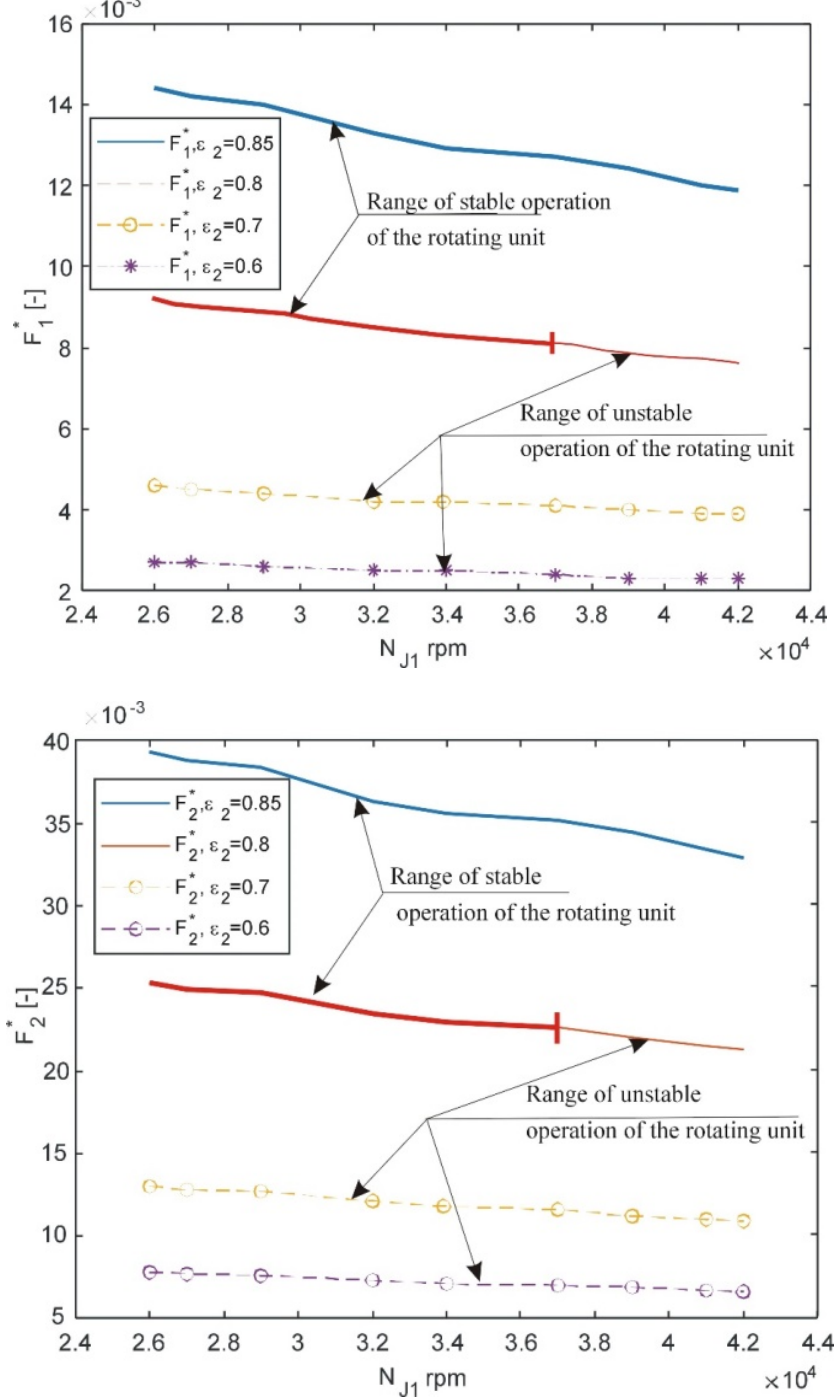


Fig. 5. Influence of rotational speed of the rotating assembly and relative eccentricity on the dimensionless load of slide bearings with a floating ring

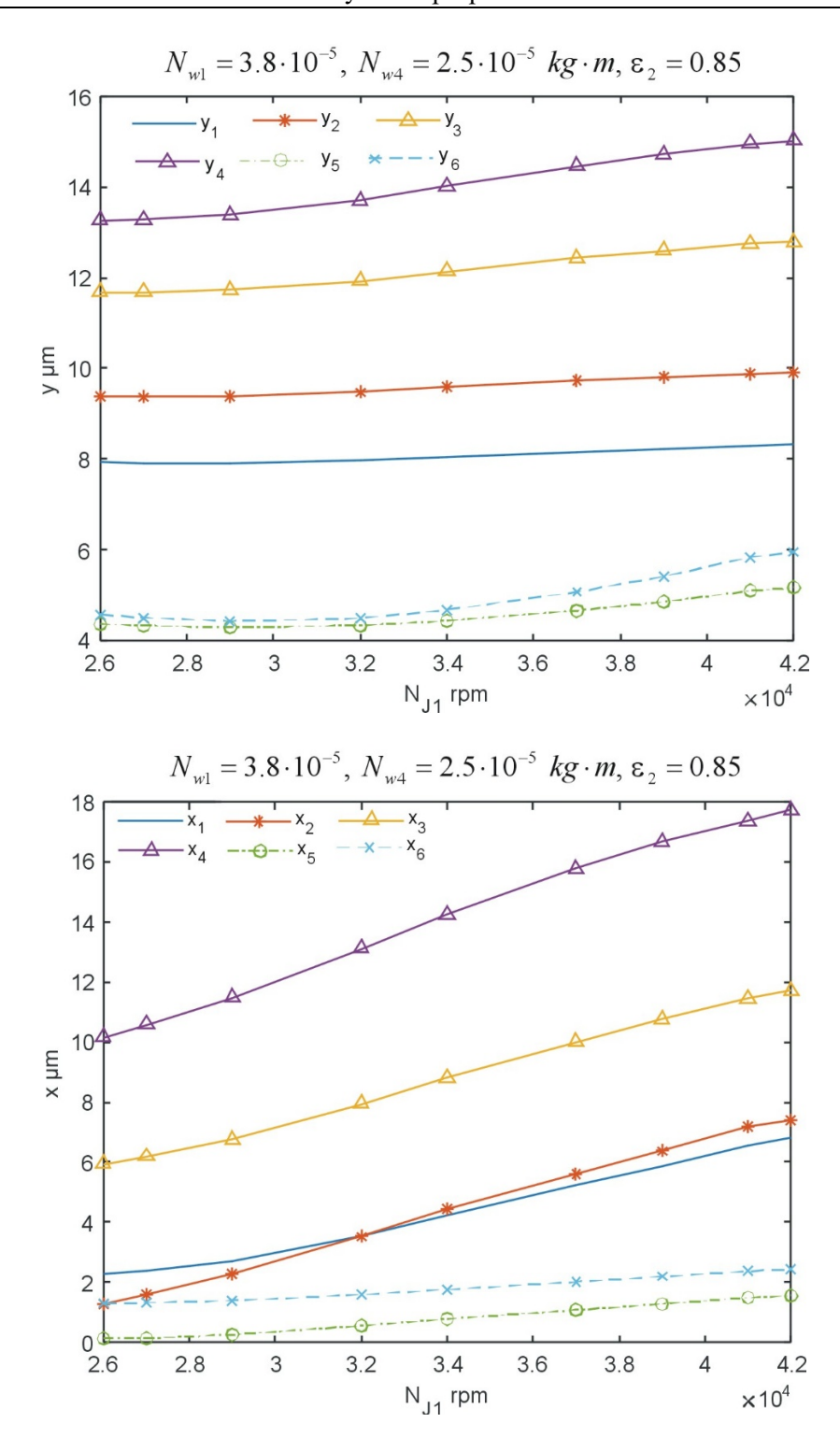


Fig. 6. Influence of the rotational speed and imbalance of the rotating assembly on vibration displacement amplitudes in the direction of the x and y coordinates in the structural nodes of the rotating assembly for imbalance on the turbine side  $N_{w1} = 3.8 \cdot 10^{-5} \ kgm$  and the compressor side  $N_{w4} = 2.5 \cdot 10^{-5} \ kgm$ 

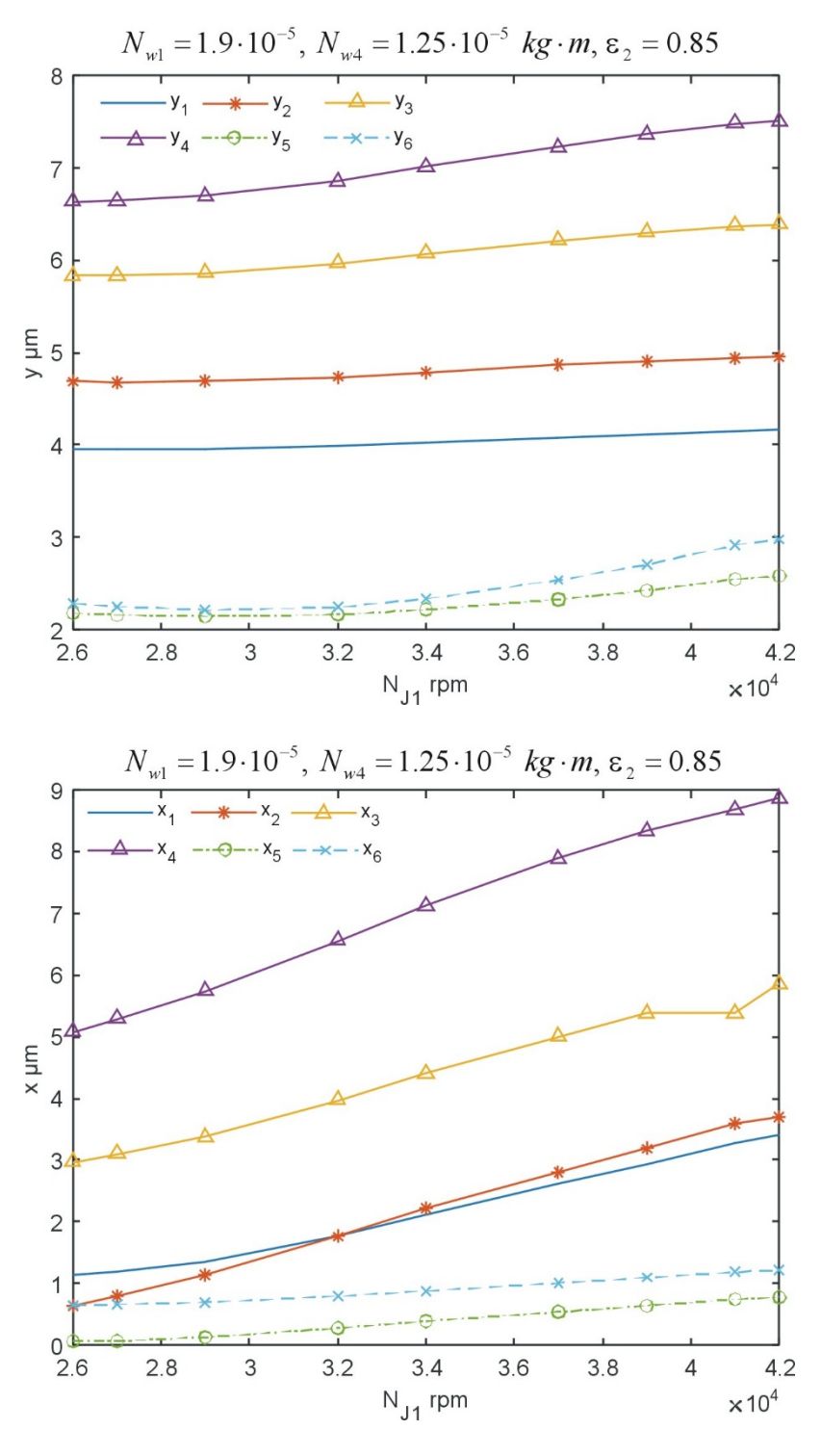


Fig. 7. Influence of the rotational speed and imbalance of the rotating assembly on vibration displacement amplitudes in the direction of the x and y coordinates in the structural nodes of the rotating assembly for imbalance on the turbine side  $N_{w1} = 1.9 \cdot 10^{-5} \ kgm$  and the compressor side  $N_{w4} = 1.25 \cdot 10^{-5} \ kgm$ 

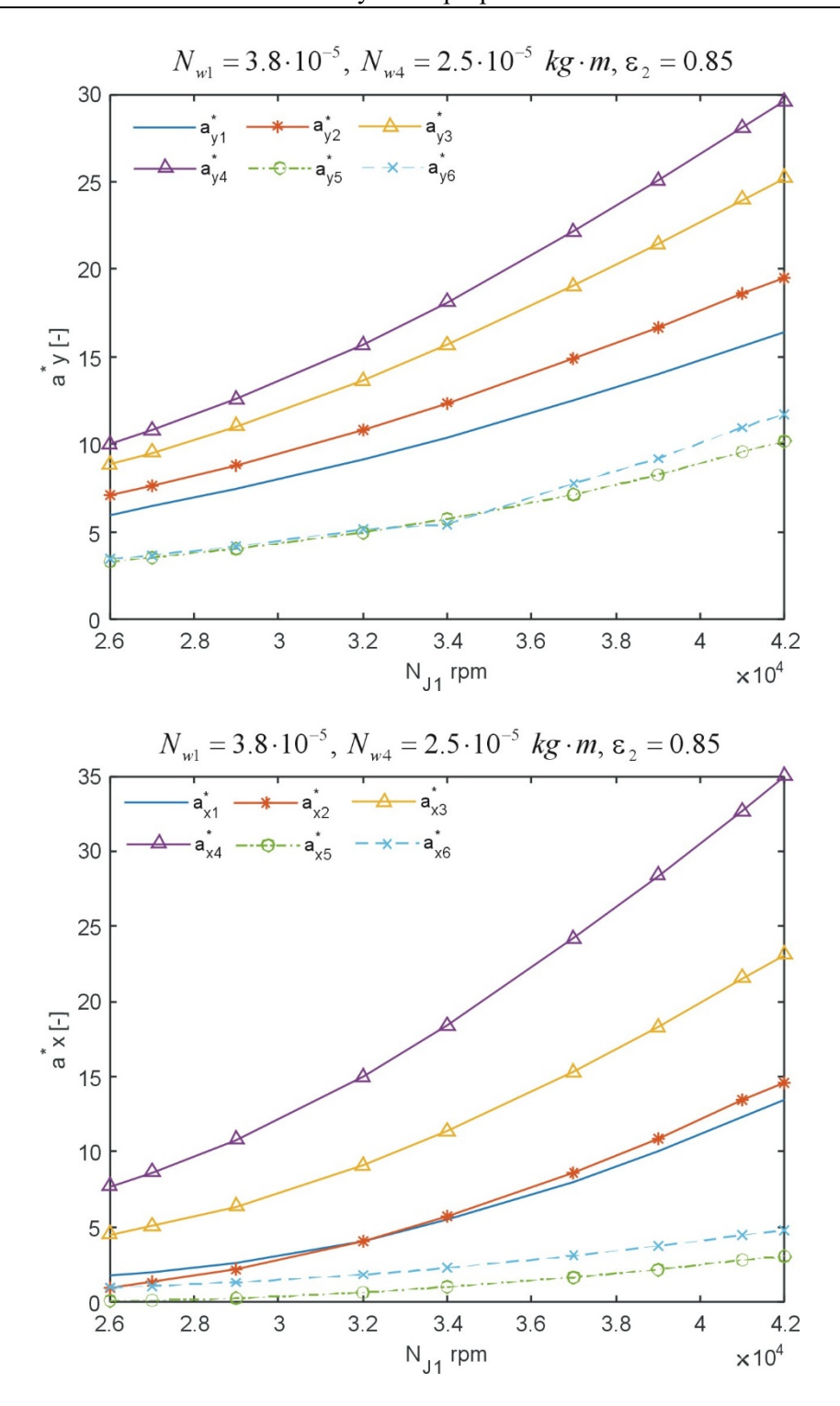


Fig. 8. Influence of the rotational speed and imbalance of the rotating assembly on the amplitudes of vibration accelerations in the *x* and *y* direction in the rotating assembly nodes for the imbalance on the turbine side  $N_{w1} = 3.8 \cdot 10^{-5} \ kgm$  and the compressor side  $N_{w4} = 2.5 \cdot 10^{-5} \ kgm$ 

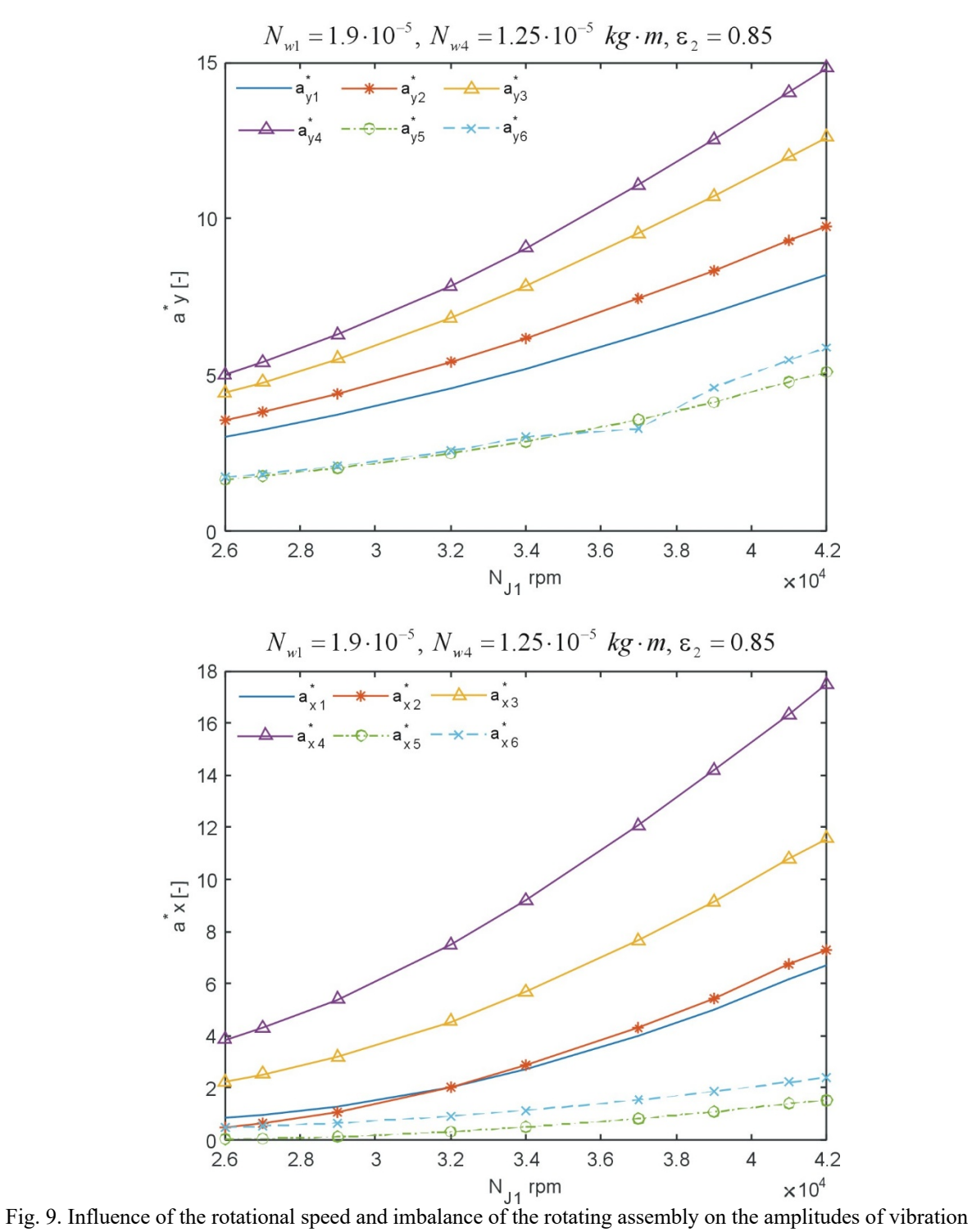


Fig. 9. Influence of the rotational speed and imbalance of the rotating assembly on the amplitudes of vibration accelerations in the x and y direction in the rotating assembly nodes for the imbalance on the turbine side  $N_{w1} = 1.9 \cdot 10^{-5} \ kgm$  and the compressor side  $N_{w4} = 1.25 \cdot 10^{-5} \ kgm$ 

# 5. CONCLUSIONS

A review of the available literature revealed that a turbocharger combined with an injection system significantly impacts the performance and reliability of the main and auxiliary engines of marine vessels.

This phenomenon can be explained by the specific operating parameters of marine engines, which are usually operated at low and variable loads. This leads to incomplete fuel combustion in the cylinders, which, in turn, has several subsequent effects on the turbocharging system. These include erosion, reduced performance and efficiency of the turbocharger, loss of stability in the mechanical system, and vibrations that accelerate bearing wear and fatigue cracks in the rotor blades. These problems confirm that a research gap still exists in this area and that the research presented by the authors remains highly relevant and necessary.

The present study demonstrates the impact of vibration damping in sliding bearings with a floating ring on the operation of an imbalanced turbocharger rotating assembly. The research was conducted on a rotating assembly in which the masses of the turbine and compressor rotors were configured asymmetrically in accordance with the technical documentation of the turbocharger. The operating parameters of the rotating assembly were calculated for different imbalance values between the turbine and compressor rotors. Due to the materials used, the authors assumed different masses of the turbine and compressor rotors and used an adiabatic heat transfer model to calculate the bearing operating parameters. The results of the numerical calculations show a high degree of agreement with the tests carried out on a test bench.

A comparative analysis of the calculated values of displacement and vibration acceleration of the rotating assembly indicates that bearings with floating rings effectively dampen the vibroacoustic effects accompanying the operation of the rotating assembly:  $x_{5,6} << x_{1,4}$  and  $y_{5,6} << y_{1,4}$  and  $a_{x5,6}^* << a_{x1,4}^*$  and

$$a_{y5,6}^* << a_{y1,4}^*$$

It was also noted that turbocharger failures can be caused by the excessive imbalance of the rotating assembly, which was confirmed by the results of braking tests. At high imbalance values of  $N_{w1}$ =3.8,  $N_{w4}$ =2.5kg·m, a significant increase in vibration displacement amplitudes was observed in the turbine and compressor rotors. Excessive increases in these amplitudes can lead to contact between the turbine and compressor rotors and the housing, which can also result in turbocharger failure.

The inclusion of the presented test results in the turbocharger design process is believed to improve the durability and reliability of turbochargers, which is significant in the context of marine propulsion systems.

Furthermore, in the authors' opinion, this research offers a promising approach to addressing specific challenges, including those related to the imbalance and dynamic properties of rotating turbocharger assemblies. This area of research will undoubtedly require further analysis and testing, including assessments of the durability of the propulsion system in light of the problems associated with operating turbochargers in marine conditions.

### References

- 1. Charchalis, A. Wielosymptomowy system diagnozowania okrętowych turbinowych silników spalinowych. *Diagnostyka*. 2004. Vol. 30. P. 101-105. [In Polish: Multi-symptom diagnostic system for marine gas turbine engines. *Diagnostics*].
- Knežević, V. & Orović, J. & Stazić, L. & Čulin, J. Fault tree analysis and failure diagnosis of marine diesel engine turbocharger system. *Journal of Marine Science and Engineering*. 2020. Vol. 8(12). No. 1004.
- 3. Korczewski, Z. Badania diagnostyczne okrętowych tłokowych silników spalinowych. *Zeszyty Naukowe Akademii Marynarki Wojennej*. 2004. Vol. 45. P. 57-72. [In Polish: Diagnostic tests of marine piston combustion engines. *Scientific Papers of the Naval Academy*].
- 4. Buluschek, B. *Das Schwimmbüchsenlager bei stationärem Betrieb*. Doctoral Thesis. ETH Zurich. 1980. Available at: https://www.research-collection.ethz.ch/handle/20.500.11850/136969. [In German: *The Floating Sleeve Bearing During Stationary Operation*].
- 5. Clarke, D.M. & Fall, C. & Hayden, G.N. & Wilkinson, T.S. A steady-state model of a floating ring bearing, including thermal effects. *Journal of Tribology*. 1992. Vol. 114(1). P. 141-149.

- 6. Someya, T. Journal-Bearing Databook. Springer Science & Business Media. 2013. 336 p.
- 7. Zhang, Y. & Yang, L. & Li, Z. & Yu, L. Research on static performance of hydrodynamically lubricated thrust slider bearing based on periodic harmonic. *Tribology International*. 2016. Vol. 95. P. 236-244.
- 8. Mazurkow, A. *Teoria smarowania łożysk ślizgowych*. Rzeszów: Oficyna Wydawnicza Politechniki Rzeszowskiej. 2019. [In Polish: *Theory of lubrication of sliding bearings*. Rzeszow: Publishing House of the Rzeszow University of Technology].
- 9. Bertz, W.J. Synthetische Hydraulikflüssigkeiten für Hochleistungsanwendungen ein Überblick. 2000. [In German: Synthetic hydraulic fluids for high-performance applications an overview].
- 10. Mazurkow, A. *Właściwości Statyczne i Dynamiczne, Metoda Projektowania Łożysk Ślizgowych z Panewką Pływającą*. Oficyna Wydawnicza Politechniki Rzeszowskiej. 2009. [In Polish: *Static and Dynamic Properties, Design Method for Floating Bearings*. Publishing House of the Rzeszów University of Technology].
- 11. Jakeman, R.W. Performance and oil film dynamic coefficients of a misaligned sterntube bearing. *ASLE Transactions*. 1986. Vol. 29(4). P. 441-450. DOI: 10.1080/05698198608981706.
- 12. Tamunodukobipi, D. & Ho Kim, C. & Lee, Y.B. Dynamic performance characteristics of floating-ring bearings with varied oil-injection swirl-control angles. *Journal of Dynamic Systems, Measurement, and Control.* 2014. Vol. 137. No. 021002. DOI: 10.1115/1.4027912.
- 13. Fischer, A. & Doikin, A. & Rulevskiy, A. Research of dynamics of the rotor with three-film bearings. *Procedia Engineering*. 2016. Vol. 150. P. 635-640.
- 14. Mazurkow, A. & Homik, W. & Lewicki, W. & Łosiewicz, Z. Evaluation of selected dynamic parameters of rotating turbocharger units based on comparative model and bench tests. *Energies*. 2023. Vol. 16(14). No. 5550.
- 15. Novotný, P. & Škara, P. & Hliník, J. The effective computational model of the hydrodynamics journal floating ring bearing for simulations of long transient regimes of turbocharger rotor dynamics. *International Journal of Mechanical Sciences*. 2018. Vol. 148. P. 611-619.
- 16. Smolík, L. & Dyk, Š. Towards efficient and vibration-reducing full-floating ring bearings in turbochargers. *International Journal of Mechanical Sciences*. 2020. Vol. 175. No. 105516.
- 17. Peng L. & Zheng, H. & Shi, Z. Performance of relative clearance ratio of floating ring bearing for turbocharger-rotor system stability. *Machines*. 2021. Vol. 9(11). No. 285.

Received 07.02.2024; accepted in revised form 27.08.2025